

Accepted for publication in *Astrophysical Journal Letters*.
1999 October 4.

**NICMOS Imaging of the Dusty Microjansky Radio Source
VLA J123642+621331 at $z = 4.424$ ¹**

I. Waddington, R. A. Windhorst and S. H. Cohen

*Department of Physics and Astronomy, Arizona State University, PO Box 871504, Tempe,
AZ 85287-1504*

Ian.Waddington@asu.edu

R. B. Partridge

Department of Astronomy, Haverford College, Haverford, PA 19041

and

H. Spinrad and D. Stern

Department of Astronomy, University of California, Berkeley, CA 94720

ABSTRACT

We present the discovery of a radio galaxy at a likely redshift of $z = 4.424$ in one of the flanking fields of the Hubble Deep Field. Radio observations with the VLA and MERLIN centered on the HDF yielded a complete sample of microjansky radio sources, of which about 20% have no optical counterpart to $I \leq 25$ mag. In this Letter, we address the possible nature of one of these sources, through deep *Hubble Space Telescope* NICMOS images in the F110W (J_{110}) and F160W (H_{160}) filters. VLA J123642+621331 has a single emission line at 6595 Å, which we identify with $\text{Ly}\alpha$ at $z = 4.424$. We argue that this faint ($H_{160} = 23.9$ mag), compact ($r_e \simeq 0''.2$), red ($I_{814} - K = 2.0$) object is most likely a dusty, star-forming galaxy with an embedded active nucleus.

Subject headings: galaxies: active — galaxies: starburst — galaxies: evolution — galaxies: individual (VLA J123642+621331)

¹Based on observations with the NASA/ESA *Hubble Space Telescope* obtained at the Space Telescope Science Institute, which is operated by the Association of Universities for Research in Astronomy, Inc., under NASA contract NAS5-26555; and with the W. M. Keck Observatory, which is operated as a scientific partnership among the University of California, the California Institute of Technology, and NASA, made possible by the generous financial support of the W. M. Keck Foundation.

1. Introduction

One of the contemporary topics of interest in extragalactic astronomy is to measure the star formation history of the universe (Madau et al. 1996). However, a major uncertainty in calculating the star formation rate (SFR) is the effect of dust obscuration, particularly for measurements in the ultraviolet and at high redshifts. For example, Calzetti & Heckman (1999) found that at $z \sim 3$ even a modest amount of dust can reduce the 1500 Å flux of a galaxy by a factor of 5. This is of particular significance for the high- z evolution of the SFR: does the SFR turn over at $z \sim 1.5$ as Madau et al. (1996) suggested, or is it constant (or even increasing) for $z \gtrsim 1.5$ (e.g. Pascarelle, Lanzetta, & Fernández-Soto 1998; Steidel et al. 1999)? If a high-redshift starburst is *significantly* reddened by dust, then its ultraviolet flux will be so obscured that it will have a negligible Lyman-limit break. Such sources would not have been detected by Steidel et al. (1999), and their measurements of the SFR could still be under-estimating the actual amount of star formation at high- z .

A powerful technique to avoid the problem of dust obscuration is to use radio-selected galaxies as probes of the star formation history (Cram 1998). The most important advantage of this technique is that radio emission is not attenuated by dust and thus a radio-selected sample is unbiased with respect to dust, unlike the optical/infrared selection techniques that are widely used. Haarsma et al. (1999) conclude from their study that the radio-selected SFR is somewhat higher than the Madau et al. (1996) results for $z < 1$, even when the latter have been corrected for dust. At higher redshifts, the “radio Madau diagram” is poorly constrained but is consistent with a relatively constant or increasing star formation rate. This suggests that a significant fraction of the star formation in the universe may be obscured by dust.

Radio-selected samples thus provide an essential tool for understanding the cosmic history of dust, as well as of the SFR. In particular, radio sources that are heavily reddened in the optical (restframe ultraviolet at redshifts of interest) can be used to constrain the dust content of high- z galaxies. We present in this Letter deep *HST*/NICMOS images of the microjansky radio source VLA J123642+621331. At a probable redshift of 4.424, this is the second highest redshift radio-selected galaxy currently known. It was barely detected in the reddest optical wavebands and is an excellent candidate for a dusty high- z galaxy.

We use a cosmology with $H_0 = 65 \text{ km s}^{-1} \text{ Mpc}^{-1}$, $\Omega_M = 0.2$ and $\Omega_\Lambda = 0$ throughout. All magnitudes are in the AB system, unless noted otherwise. For comparison, Vega-based magnitudes are approximately given by: $I_{814} - 0.4$, $J_{110} - 0.7$, $H_{160} - 1.3$, $K - 1.9$, and $(I_{814} - K) + 1.5$.

2. VLA J123642+621331

Two of the deepest high-frequency radio surveys available are those centered on the Hubble Deep Field (Richards et al. 1998; Richards 2000) and the Small Selected Area 13 (Windhorst et al. 1995). These surveys reach 5σ detection limits of $8 \mu\text{Jy}$ at 8.5 GHz (HDF and SSA13) and $40 \mu\text{Jy}$

at 1.4 GHz (HDF). Optical identifications of the sources were made on deep *Hubble Space Telescope* and ground-based images, primarily in the I-band. Approximately 20% of the 1.4 GHz sources were not identified, although a few of them show faint optical emission below the formal completeness limit of the I-band images. The full sample is discussed by Richards et al. (1999); in this Letter we investigate in detail one of these “unidentified” sources.

VLA J123642+621331 is a steep-spectrum radio source ($\alpha = 0.94 \pm 0.06$) with flux densities of $70 \mu\text{Jy}$ at 8.5 GHz and $470 \mu\text{Jy}$ at 1.4 GHz (Richards et al. 1998; Richards 2000). Approximately 10% of its radio flux density is extended in an eastward jet in $0''.15$ MERLIN observations, with the remainder in a resolved compact core (Muxlow et al. 1999). The source was identified with a faint object below the formal completeness limit of the HDF Flanking Field I-band image (IW3), with a magnitude of $I_{814} = 25.3 \pm 0.2$ (Figure 1a). The object was also identified in the K-band image of Dickinson (1998) from the KPNO 4-meter telescope, and has a magnitude of $K = 23.25 \pm 0.05$ (Figure 1d). The KPNO images do not detect the object in either the J or H bands. Aussel et al. (1999) identify VLA J123642+621331 in their supplementary list of sources detected by ISOCAM on the Infrared Space Observatory. It has a flux of $23_{-12}^{+10} \mu\text{Jy}$ in the LW3 filter at $15 \mu\text{m}$, corresponding to an AB magnitude of 20.5 ± 0.5 . The source lies at the edge of the SCUBA sub-millimeter map of Hughes et al. (1998) and was not detected, giving a conservative upper limit of 5 mJy to its $850 \mu\text{m}$ flux.

3. NICMOS Observations & Processing

In December 1997, we observed VLA J123642+621331 with the *Hubble Space Telescope* NICMOS camera 2 for three orbits in F110W (close to the J-band) and six in F160W (essentially the H-band), in the Continuous Viewing Zone. In each orbit, five 1024-second exposures were taken using a spiral dither pattern with $1''.3$ offsets. We reduced the images using a two stage process: first we ran them through the standard pipeline CALNICA, using the most recent calibration files, and then we applied a further flat-field correction to the data, adapted from standard ground-based infrared imaging methods.

Following CALNICA processing, additional bad pixels were flagged after a visual inspection of the data — these consisted of a dead column, the coronagraph hole and other insensitive pixels (also known as the “grot”). Since the NICMOS camera actually consists of four physically separate sub-arrays, we obtained better results by dividing each partially-reduced image into four separate quadrants. For each filter, all the exposures of each quadrant were stacked and a median image calculated. Given that the exposures were dithered by $1''.3$, this produced a map of the residual instrumental features, devoid of any astronomical objects — a “super-sky”. The super-sky images for each quadrant were normalized to the mean of all four quadrants in order to preserve the quadrant-to-quadrant photometric accuracy. Each exposure was then *divided* by this normalized super-sky. We also tested the results of *subtracting* a scaled copy of the super-sky from each exposure and found that the results were not significantly different (the standard deviation of

an empty sky region varied randomly by less than 3% between the two methods). The success of this super-sky division suggests that the instrumental features left after CALNICA processing were most likely due to differences between the sky and the calibration flat-fields, rather than poor subtraction of the bias or dark current. Finally, all the quadrants were combined to produce F110W and F160W mosaics. By ensuring that the mean of our super-sky was unity, the overall sensitivity of the images was unchanged by the additional processing and they were calibrated using the most recent photometric calibration parameters from STScI.

Figure 1c shows the 6-orbit NICMOS image in F160W. The counterpart to the radio source is clearly detected at $1.6 \mu\text{m}$, with an AB magnitude of $H_{160} = 23.87 \pm 0.04$ in a 1.5 arcsec diameter circular aperture. The 3-orbit NICMOS image in F110W provided a marginal detection of $J_{110} = 25.2 \pm 0.4$ (Figure 1b). Thus the object is very red with $(I_{814} - K) = 2.0 \pm 0.2$, $(J_{110} - H_{160}) = 1.3 \pm 0.4$ and $(H_{160} - K) = 0.6 \pm 0.1$.

4. Keck Observations

We obtained spectra of VLA J123642+621331 through $1''.5$ wide, $\approx 30''$ long slits using the LRIS spectrograph (Oke et al. 1995) at the Keck II telescope in slitmask mode. On UT 1998 February 19, with $0''.8$ seeing and photometric conditions, we observed VLA J123642+621331 for 1.9 hr (position angle 103°) with the 400 lines mm^{-1} grating, sampling the wavelength range 5700–9400 Å, at $\Delta\lambda_{\text{FWHM}} \approx 11$ Å. On UT 1999 May 10, with $0''.6$ seeing and thin cirrus, we observed the source for 2 hr (position angle -67°) with the 150 lines mm^{-1} grating, with $\Delta\lambda_{\text{FWHM}} \approx 17$ Å resolution over the wavelength range 4000 Å to $1 \mu\text{m}$. Between each 1800 s exposure, we performed a $\sim 4''$ spatial shift along the slit to facilitate removal of fringing in the reddest regions of the spectra. Final wavelength calibration is accurate to better than 1 Å.

There is a strong, single emission line at $\lambda \simeq 6595$ Å *in both data sets*, which we identify with Ly α at a redshift of 4.424 (Figure 2, Table 1). The line shifts by ≈ 7 Å between the two observations, which corresponds to a velocity difference of 320 km s^{-1} if it is due to a Doppler shift. In both years' data, the line was offset by $\approx 1''$ to the north-west of the (marginal) I-band detection. Emission-line regions of high-redshift radio galaxies are known to be kinematically complex (Chambers, Miley, & van Breugel 1990; van Ojik et al. 1997), thus slight pointing changes between the two observations may have caused the slit to sample different regions of spatially-extended, line-emitting gas.

5. Discussion

The only two reasonable identifications for the single emission line are Ly α or [O II] 3727. We argue that it is unlikely to be [O II] at $z = 0.77$ for the following reasons. The faint K magnitude of 23.3 argues strongly against the source being at low- z when it is compared to the K- z relation of radio galaxies (see van Breugel et al. 1999 for a recent version). If VLA J123642+621331 were

at $z = 0.77$, it would be 3–4 magnitudes underluminous in K compared with all other known radio galaxies at that redshift. The restframe equivalent width if the line were [O II] would be $W_{[\text{OII}]}^{\text{rest}} > 207 \text{ \AA}$, which is very large for [O II]. The absence of a redshifted [O III] doublet at $\sim 8860 \text{ \AA}$ further argues against $z = 0.77$, although this argument is not completely satisfying as galaxies show a wide range in [O III]/[O II] ratios and our flux limits are not particularly strong.

The alternative is to identify the emission line with Ly α at $z = 4.424$. We compared the observed SED from $0.8 \mu\text{m}$ to $15 \mu\text{m}$ with the 1996 revision of the spectral evolution models of Bruzual & Charlot (1993). We used a single burst model of solar metallicity and added a foreground screen of dust, modeling the effects of dust obscuration with the extinction law of Calzetti, Kinney, & Storchi-Bergmann (1994). The best-fitting model we obtain has an age of $(1.6 \pm 1.0) \times 10^7$ years with $A(V) = 1.6 \pm 0.3$ mag (Figure 3). No model of any age is able to reproduce the red colors of this galaxy with $A(V) < 0.5$ mag at the 99.99% confidence level. The results are essentially independent of the metallicity, from 0.02 of solar to solar. We note that the models predict a $15 \mu\text{m}$ flux that is too faint, although given the large ISO errors the models were consistent to within $\lesssim 2\sigma$. We also attempted to fit the galaxy with a model spectrum at $z = 0.77$ and were unable to obtain *any* acceptable fit to the optical/near-infrared SED: the minimum χ^2 was ~ 30 for a 18 Gyr model with no dust extinction, compared with a χ^2 of 2.5 for the best-fitting $z = 4.424$ model. In particular, the low redshift models could not reproduce the red H $_{160}$ – K color of 0.6 ± 0.1 , nor did they fit the $15 \mu\text{m}$ flux.

The sub-millimeter ($850 \mu\text{m}$) to radio (1.4 GHz) spectral index has recently been used by Carilli & Yun (1999) as a redshift indicator. With a spectral index of $\alpha_{1.4}^{353} \geq -0.4$ ($S_\nu \propto \nu^{-\alpha}$), VLA J123642+621331 is consistent with this correlation at either $z = 0.77$ for a starburst galaxy, or at $z = 4.424$ if the 1.4 GHz flux is dominated by an AGN. Thus the current SCUBA sub-millimeter detection limit does not favor either a high or low redshift interpretation. The lack of a far-infrared/sub-millimeter detection prevents us from drawing conclusions about the emission properties of the dust that must be present based on the reddening of the optical/infrared SED.

We note that it is possible that we detected a serendipitous $z = 4.42$ background object in the Keck spectra, that is not associated with the radio source. We used the number counts and redshift distribution of galaxies in the HDF to find the random probability that a $z > 4$ source with a magnitude 1–2 mag below the completeness limit of the I-band image would be found within a $1''$ radius of the optical identification. From this calculation we estimate that there is a probability of $\lesssim 10^{-3}$ that the spectra are of a background source.

The surface brightness profile of VLA J123642+621331 was produced by fitting elliptical isophotes to the F160W image (Figure 4). We extracted model surface brightness profiles from an ensemble of two-dimensional exponential and de Vaucouleurs models convolved with a model PSF from “Tiny Tim”. The best-fitting model is an exponential with scale-length $r_e = 0''.17 \pm 0''.02$ (where $I \propto e^{-r/r_e}$) or 1.4 ± 0.2 kpc in our chosen cosmology. Any unresolved point source (i.e., an AGN) contributes $\lesssim 10\%$ of the total flux in the H-band. A de Vaucouleurs $r^{1/4}$ profile does not fit the data.

We note briefly the contrast between the dominant exponential profile of VLA J123642+621331 and the profiles of other very red high- z sources, of which several are now known at $z \simeq 1.5$ –2 that have regular $r^{1/4}$ profiles (e.g., Stiavelli et al. 1999, Waddington et al. 1999).

It can be seen in Figure 1 that there is some two-dimensional structure to the galaxy. It is extended in a roughly north–south direction in the F160W image, perpendicular to the radio jet. In the F814W image there is a faint hint of extended emission to the west of the radio position, in the opposite direction to the radio jet but aligned with the Ly α emission. The marginal J-band detection may be similarly extended to the west. The apparent structure in the K-band is probably not real, but is likely due to the PSF and/or the drizzling procedure, given that other objects in the image show a similar structure. It is also possible that there is a contribution to the K-band light from redshifted [O II] 3727. Most high- z radio galaxies have distorted or aligned morphologies (e.g., Best, Longair, & Röttgering 1997) and it is an important question whether such a low power radio source as VLA J123642+621331 is also aligned with its ultraviolet/optical emission.

The preceding arguments lead us to the following interpretation. VLA J123642+621331 is a disk system at a likely redshift of $z = 4.424$, containing an embedded, weak AGN. With an 8.4 GHz luminosity of 2.0×10^{25} W Hz $^{-1}$, it is at the faint end of the radio luminosity function for AGN, intermediate between an AGN and a starburst. Both the radio jet that is visible in the MERLIN image and the sub-millimeter to radio spectral index suggest it is an AGN. The AGN must be obscured in the ultraviolet/optical, as it is not seen in either the F160W profile or in the colors of the SED. The observed Ly α luminosity of 2×10^{42} erg s $^{-1}$ (Table 1) is a factor of 10–100 fainter than typical high-redshift radio galaxies (Röttgering et al. 1997), and its Ly α line-width (FWHM $\simeq 440$ km s $^{-1}$) is 2–3 times narrower than the other known $z > 4$ radio galaxies (van Breugel et al. 1999).

The galaxy underwent a burst of star formation approximately 16 million years before we observe it, although the presence of dust suggests that this was not the first starburst. It is a dusty galaxy with an extinction of 1.6 mag in the visual, and a corresponding ultraviolet extinction of $A(1216 \text{ \AA}) \simeq 4$ mag. This would be sufficient to render any Ly α emission *from the disk* undetectable in our Keck spectrum, if it were of comparable intrinsic luminosity to the (unreddened) line that we do observe. The Ly α emission line came from an extended region about 1'' to the north-west of the galaxy, roughly aligned with the radio axis. This Ly α emission region could be an infalling gas cloud that is either scattering/reradiating Ly α from the AGN into our line of sight, or is the site of recent (jet-induced) star formation. Such extended Ly α clouds have been observed around several high-redshift AGN at $z \simeq 2.4$ (Francis, Woodgate & Danks 1997; Windhorst, Keel, & Pascarella 1998; Keel et al. 1999) and we should perhaps expect such structures to be more abundant at higher redshifts, where the gas has had less time to collapse. Deep imaging of the source at $\sim 6600 \text{ \AA}$ is needed in order to investigate the nature of this cloud.

We thank Eric Richards, Ken Kellerman, Ed Fomalont and Tom Muxlow for useful discussions and for sharing unpublished data; Andy Bunker for contributing to the Keck observations; and

Mark Dickinson for making his KPNO infrared observations of the HDF publicly available. This work was supported by NASA grant GO-7452.0*.96A from STScI under NASA contract NAS5-26555, and by NSF grant AST9802963.

REFERENCES

- Aussel, H., Cesarsky, C. J., Elbaz, D., & Starck, J. L. 1999, *A&A*, 342, 313
- Best, P. N., Longair, M. S., & Röttgering, H. J. 1997, *MNRAS*, 292, 758
- Bruzual A., G., & Charlot S. 1993, *ApJ*, 405, 538
- Cazetti, D., & Heckman, T. M. 1999, *ApJ*, 519, 27
- Calzetti, D., Kinney, A. L., & Storchi-Bergmann, T. 1994, *ApJ*, 429, 582
- Carilli, C. L., & Yun, M. S. 1999, *ApJ*, 513, L13
- Chambers, K., Miley, G., & van Breugel, W. 1990, *ApJ*, 363, 21
- Cram, L. 1998, *ApJ*, 506, L85
- Dickinson, M. 1998, in *The Hubble Deep Field*, eds. M. Livio, M. Fall, & P. Madau, Cambridge Univ. Press, p. 219
- Francis, P. J., Woodgate, B. E., & Danks, A. C. 1997, *ApJ*, 482, L25
- Haarsma, D. B., et al. 1999, in preparation
- Hughes, D. H., et al. 1998, *Nature*, 394, 241
- Keel, W. C., Cohen, S. H., Windhorst, R. A., & Waddington, I. 1999, *AJ*, in press (December 1999)
- Madau, P., Ferguson, H. C., Dickinson, M. E., Giavalisco, M., Steidel, C. C., & Fruchter, A. 1996, *MNRAS*, 283, 1388
- Muxlow, T., et al. 1999, in preparation
- Oke, J. B., et al. 1995, *PASP*, 107, 375
- Pascarelle, S. M., Lanzetta, K. M., Fernández-Soto, A. 1998, *ApJ*, 508, L1
- Richards, E. A. 2000, *ApJ*, in press
- Richards, E. A., Fomalont, E. B., Kellerman, K. I., Partridge, R. B., Windhorst, R. A., Cowie, L. L., & Barger, A. J. 1999, *ApJ*, this volume
- Richards, E. A., Kellermann, K., Fomalont, E., Windhorst, R., & Partridge, R. 1998, *AJ*, 116, 103

- Röttgering, H., van Ojik, R., Chambers, K., van Breugel, W., & de Koff, S. 1997, *A&A*, 326, 505
- Steidel, C. C., Adelberger, K. L., Giavalisco, M., Dickinson, M., & Pettini, M. 1999, *ApJ*, 519, 1
- Stiavelli, M., et al. 1999, *A&A*, 343, L25
- van Breugel, W., de Breuck, C., Stanford, S. A., Stern, D., Röttgering, H., & Miley, G. 1999, *ApJ*, 518, L61
- van Ojik, R., Röttgering, H. J. A., Miley, G. K., & Hunstead, R. W. 1997, *A&A*, 317, 358
- Waddington, I., Windhorst, R. A., Peacock, J. A., Dunlop, J. S., Cohen, S. H., & McClure, R. 1999, in preparation
- Windhorst, R. A., et al. 1995, *Nature*, 375, 471
- Windhorst, R. A., Keel, W. C., & Pascarelle, S. M. 1998, *ApJ*, 494, L27

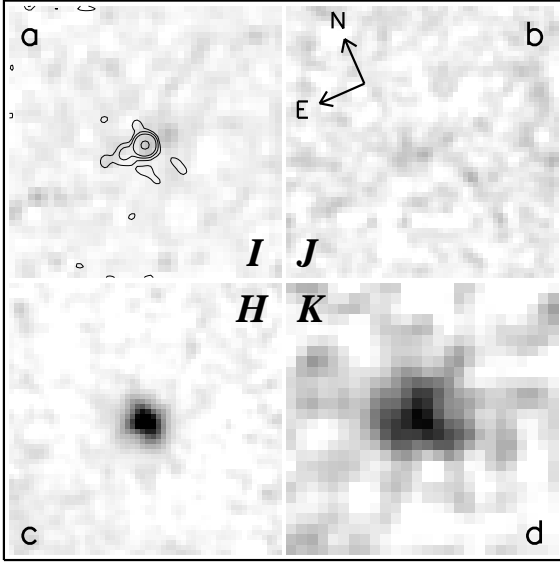


Fig. 1.— Multiband images of VLA J123642+621331. (a) WFPC2 F814W (I-band) grey-scale image, overlaid with the 1.4 GHz combined (uniform weighted) MERLIN/VLA radio image of Muxlow et al. (1999), at a resolution of approximately 0.15 arcsec. Contour levels are at flux densities of 8, 16, 32, 128 μJy ($\sigma = 4 \mu\text{Jy}$). (b) The source is barely detected in a 3-orbit NICMOS F110W (J-band) image. (c) The 6-orbit NICMOS F160W (H-band) image shows a very red object at the radio position. (d) Ground-based K-band image with the KPNO 4-meter ($1''.0$ seeing). Each image is 4 arcsec on a side and has been smoothed with a 2-pixel wide gaussian.

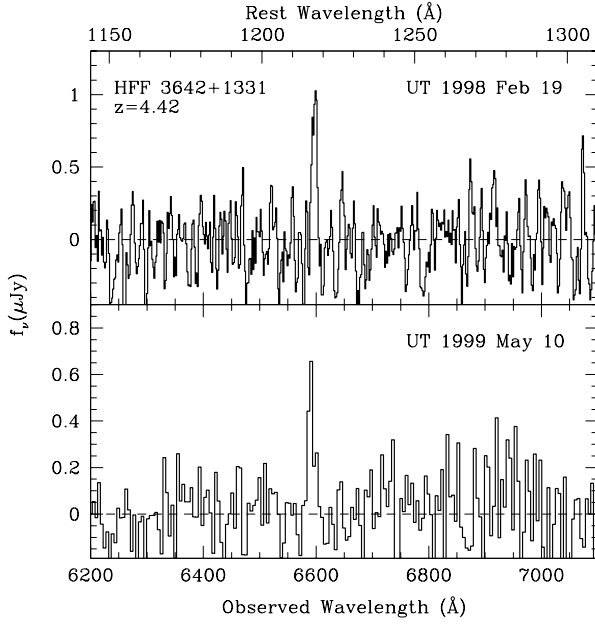


Fig. 2.— Keck spectra of VLA J123642+621331. The single emission line is detected in two independent observations over a period of more than a year, and is identified as Ly α at $z = 4.424$. The 1998 spectrum is smoothed with a 3-pixel boxcar filter.

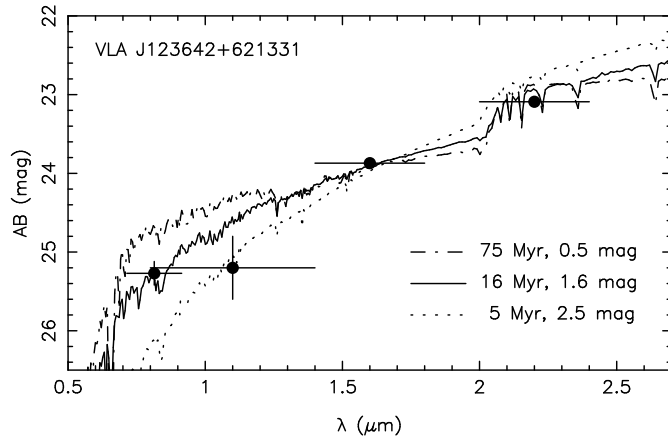


Fig. 3.— Optical/infrared spectral energy distribution of the radio galaxy. The three spectra are the best-fitting model (solid line), the oldest & least dusty model (dot-dash line) and youngest & most dusty model (dotted line), both at the $3\text{-}\sigma$ confidence limits.

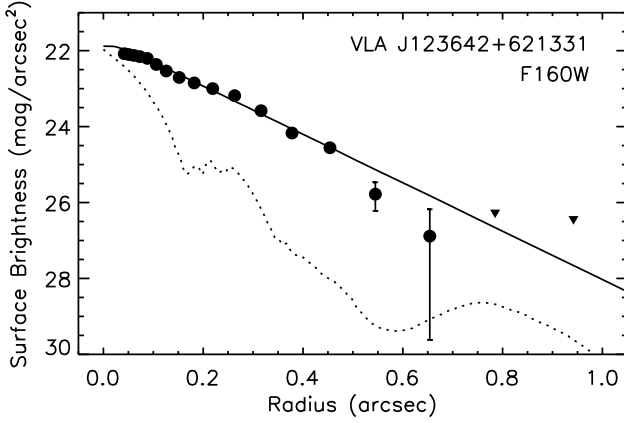


Fig. 4.— The NICMOS F160W surface brightness profile of VLA J123642+621331. Triangles denote $1\text{-}\sigma$ upper limits. The best-fitting model (solid line) is an exponential with scale-length $0''.17$ (1.4 kpc), convolved with the appropriate PSF (dotted line) from “Tiny Tim”.

Table 1. Spectroscopic Measurements

Parameter	UT 1998 Feb 19	UT 1999 May 10
z	4.427 ± 0.001	4.421 ± 0.001
λ (\AA)	6597.4 ± 1.0	6590.4 ± 1.1
$F_{\text{Ly}\alpha}$ (10^{-17} erg cm^{-2} s^{-1})	0.74 ± 0.14	0.48 ± 0.11
$F_{\lambda}^{\text{cont}}$ (10^{-21} erg cm^{-2} s^{-1} \AA^{-1})	-0.2 ± 7.3	8.4 ± 4.8
$W_{\text{Ly}\alpha}^{\text{obs}}$ (\AA)	> 483	> 249
$\text{FWHM}_{\text{Ly}\alpha}$ (km s^{-1})	420 ± 75	464 ± 155
$L_{\text{Ly}\alpha}$ (10^{42} erg s^{-1})	2.4 ± 0.4	1.5 ± 0.4